Nanomaterials

Controlled Doping of MS$_2$ (M = W, Mo) Nanotubes and Fullerene-like Nanoparticles**

*Lena Yadgarov, Rita Rosentsveig, Gregory Leitus, Ana Albu-Yaron, Alexey Moshkovich, Vladislav Perfilyev, Relja Vasic, Anatoly I. Frenkel, Andrey N. Enyashin, Gotthard Seifert, Lev Rapoport, and Reshef Tenne**

Doping of semiconductor nanocrystals and nanowires with minute amounts of foreign atoms plays a major role in controlling their electrical, optical, and magnetic properties.[1] In the case of carbon nanotubes, subsequent doping with oxygen and potassium leads to a p-type and n-type behavior, respectively.[1a–c] In another work, VO$_x$ nanotubes were transformed from spin-frustrated semiconductors to ferromagnets by doping with either electrons or holes.[2]

Calculations indicated that n- and p-type doping of multiwall MoS$_2$ nanotubes (INT) could be accomplished by substituting minute amounts of the Mo lattice atoms with either Nb[3] (p-type) and Re[4] (n-type), respectively. Substituting ($<$ 0.1 at%) molybdenum by rhenium atoms[5] and

sulfur by halogen atoms[6] was shown to produce n-type conductivity in MoS$_2$ crystals.

To synthesize rhenium-doped nanoparticles (NP) and nanotubes both in situ and subsequent doping methods were used. Figure 1a shows the quartz reactor used for in situ synthesis of rhenium doped MoS$_2$ NP with fullerene-like structure (Re:IF-MoS$_2$). The formal Re concentration was varied from 0.02 to 0.7 at%. The precursor Re$_x$Mo$_{1-x}$O$_3$ ($x < $ 0.01) powder was prepared in a specially designed auxiliary reactor (see Supporting Information). Evaporation of this powder takes place in area 1 at 770°C (Figure 1a). The oxide vapor reacts with hydrogen gas in area 2 (Figure 1a) at 800°C which leads to a partial reduction of the vapor and its condensation into Re-doped MoO$_{3-y}$ nanoparticles. The resulting NP react with H$_2$/H$_2$S gas in area 3 at 810–820°C to produce reduced oxide nanoparticles engulfed with a few closed layers of Re:MoS$_2$, which protect it against ripening into bulk 2H-MoS$_2$.[7] To complete this oxide to sulfide conversion a long (25–35 h) annealing process at 870°C in the presence of H$_2$S and forming gas (H$_2$ 10 wt%; N$_2$) was performed. At the end of this diffusion-controlled process a powder of Re-doped MoS$_2$ NP with a fullerene-like (IF) structure (Re:IF-MoS$_2$) was obtained.

In addition, doping of IF-WS$_2$ NP and INT-WS$_2$ was subsequently carried out by heating the pre-prepared IF/INT in an evacuated quartz ampoule also containing ReO$_3$, or ReCl$_3$ and iodine. In the case of ReCl$_3$, both the rhenium and the chlorine atoms (substitution to sulfur atoms) served as n-type dopants.

Typical high-resolution scanning electron microscopy (HRSEM) and transmission electron microscopy (HRTEM) micrographs of the Re-doped fullerene-like NP are shown in Figure 1b. The Re:IF-MoS$_2$ consists of about 30 closed (concentric) MoS$_2$ layers. No impurity, such as oxides, or platelets (2 H) of MoS$_2$ could be found in the product powder. The line profile and the Fourier analyses (FFT) (inset of Figure 1b) show an interlayer spacing of 0.627 nm (doped). Furthermore, the layers seem to be evenly folded and closed with very few defects and cusps, demonstrating the Re-doped NP to be quite perfectly crystalline. HRTEM did not reveal any structural changes even for the samples with high Re concentration (0.71 at%). However, owing to its quasi-spherical shape and size, this analysis cannot completely rule-out the presence of a small amount of the ReS$_2$ phase in the IF NP. Figure 1c shows a typical TEM image of Re(Cl) (post synthesis) doped multiwall WS$_2$ nanotube. There is no

[*] L. Yadgarov, Dr. R. Rosentsveig, Dr. A. Albu-Yaron, Prof. R. Tenne
Department of Materials and Interfaces, Weizmann Institute
Rehovot 76100 (Israel)
E-mail: reshef.tenne@weizmann.ac.il

Dr. G. Leitus
Department of Chemical Research Support, Weizmann Institute
Rehovot 76100 (Israel)

Dr. A. Moshkovich, Dr. V. Perfilyev, Prof. L. Rapoport
Department of Science, Holon Institute of Technology
P.O. Box 305, 52 Golomb St., Holon 58102 (Israel)

Dr. R. Vasic, Prof. A. I. Frenkel
Department of Physics, Yeshiva University
245 Lexington Ave, New York, NY 10016 (USA)

Dr. A. N. Enyashin
Institute of Solid State Chemistry UB RAS
Pervomayskaya Str., 91, 620990 Ekaterinburg (Russia)

Prof. Dr. G. Seifert
Physikalische Chemie, Technische Universität Dresden
Bergstrasse, 66b, 01062 Dresden (Germany)

Supporting information for this article is available on the WWW under http://dx.doi.org/10.1002/anie.201105324.
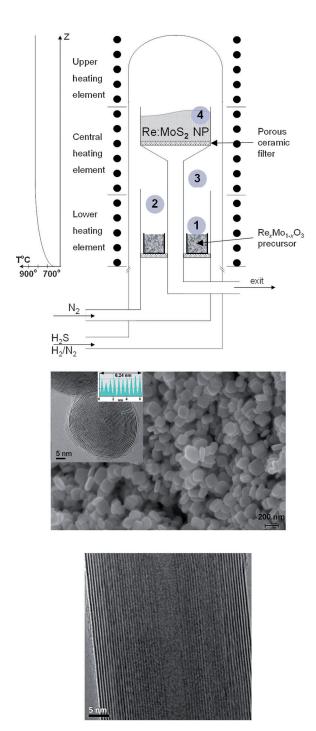
Figure 1. a) Modified quartz reactor used for the synthesis of the Re:IF-MoS$_2$ NP with the temperature profile shown along the reactor (z) axis, on the left, see text for details. b) HRSEM and HRTEM (inset) images of a typical Re(0.12 at%):IF-MoS$_2$ NP. The interlayer spacing as shown by the line profile of Re:IF-MoS$_2$ (0.627 nm) coincides with that of the undoped IF-MoS$_2$. c) HRTEM image of a post-synthesis Re-doped INT-WS$_2$.

distinction between this image and a typical TEM micrograph of pristine WS$_2$ nanotubes.
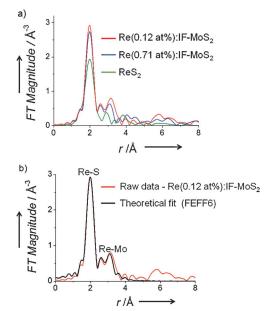
The Re concentration in the IF/INT was determined by inductive coupled plasma mass spectrometry (ICP-MS). For the Re-doped IF/INT-WS$_2$ the level of Re doping varied

between approximately 0.07–0.5 at% depending on the loading of the dopant, the temperature, and duration of the process. For the Re:IF-MoS$_2$ the Re level was found to increase with the formal ReO$_3$ content of the oxide powder and varied to some extent from one measurement to the other (three measurements for each Re concentration). These results suggested some non-uniformity in the doping level of the NP. Roughly speaking, the average Re concentration in the IF-MoS$_2$ powder was found to be about 1/3 to 1/2 of the formal (weighted) concentration in the oxide precursor. Thus in a typical nanoparticle consisting of about $5–7 \times 10^5$ Mo atoms, there are on the average about 200–300 Re atoms (in the 0.12 at% sample).

X-ray absorption fine structure (XAFS) measurements were performed to determine the dopant locations by checking the local structure around the Re atoms. Data processing and analysis of the raw X-ray absorption near edge structure (XANES) and extended XAFS (EXAFS) data were performed for IF-MoS$_2$, Re:IF-MoS$_2$ (0.12 and 0.71 at%). The Fourier transform magnitude of the data collected at the Re L$_3$ edge (Figure 2a) demonstrates distinct differences between the atomic arrangements of the Re-doped IF samples and bulk ReS$_2$. A theoretical model was constructed by replacing the X-ray-absorbing Mo atom in the MoS$_2$ structure by Re and using FEFF6 program to calculate the theoretical EXAFS contribution to Re from the first (Re–S) and second (Re–Mo) coordination shells. The good fit between the theoretical and experimental curves for the 0.12 at% sample (Figure 2b) support the substitution model for the dopant (Re$_{Mo}$).

Pure ReS$_2$ has a small Re–S first peak owing to the large first-shell disorder. Thus the larger peak intensity of the 0.12 at% Re compared to the 0.71 at% (Figure 2a) is

Figure 2. Fourier transform magnitudes of the EXAFS spectra of the Re L$_3$ edge for: a) Two Re-doped IF samples (0.12 at% red, 0.71 at% Re blue) and the ReS$_2$ (green) reference. b) Raw data (red) and theoretical fit (black) of the Re L$_3$ edge data in the 0.12 at% sample.

consistent with the 0.71 at % sample containing a small submixture of ReS_2 phase. These differences are also manifested by the interatomic distances for the different bonds between Re, S, and Mo obtained by the data analysis (Table 1). Additional detailed descriptions of the measurements and data analysis are presented in the Supporting Information. The first-shell disorder in the ReS_2 lattice reflects the fact that

Table 1: EXAFS data analysis results for the nearest neighboring (NN) bond lengths.[a]

| | ReS_2 | Bond length [Å] | | $IF\text{-}MoS_2$ |
| | | Re:$IF\text{-}MoS_2$ | | |
		0.71 at%	0.12 at%	
bond type	Re–Re	Re–Mo	Re–Mo	Mo–Mo
2NN	2.80(1)[8]	3.13(1)	3.15(1)	3.168(3)
bond type	Re–S	Re–S	Re–S	Mo–S
1NN	2.380(8)[8]	2.377(6)	2.381(7)	2.404(4)
		Mo–S	Mo–S	
		2.404(3)	2.403(4)	

[a] Uncertainties in the last digit are given in parentheses. 1NN and 2NN are first and second nearest neighbors, respectively.

there are two inequivalent Re sites, where the Re–S distances range from 2.31 to 2.50 Å. This is not the case for the Mo–Mo (or Re_{Mo}–Mo) in the MoS_2 lattice which has sixfold degenerate Mo–S bonds of 2.43 Å in length. Therefore, the XAFS data analysis also allows for quantification of the dopant solubility limit in the NP.

Doped and undoped $IF/INT\text{-}WS_2$ were also analyzed by XANES and EXAFS. The Re doping was found to induce stronger W–S bonding, and/or a less defective bonding environment. However, since the Re and W signals are almost overlapping, this method could not unequivocally confirm that Re substitute W atoms. Additional detailed descriptions of the measurements and data analysis are presented in the Supporting Information.

The limit of the rhenium solubility within the MoS_2 lattice as a dopant was estimated by using a simple thermodynamic approach (for the entropy part) and quantum mechanical calculations (for the enthalpy part). More details of the calculations are given in the Supporting Information. The results show that for a temperature around 1200 K, the maximal Re content in the MoS_2 lattice is 0.01 at %, which is somewhat below the experimentally observed value (0.02–0.05 at %). These calculations clearly indicate that the Re doping process is self-limiting, which is highly desirable for precise control of the doping densities.

To check the transport properties of the doped IF/INT compared to the undoped ones, electrical resistivity measurements of pellets compacted from their powder were carried out over a wide temperature range (Figure 3).[9] For all the IF/INT the resistivity increases with decreasing temperatures, which reflects their semiconductor behavior. Nonetheless, the doping of the IF and INT leads to a remarkable drop in their resistivity as compared to the undoped NP. The results also indicate that the resistivity decreases as the Re doping level increases.
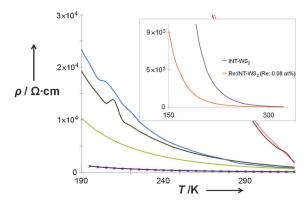

Figure 3. Resistivity versus temperature for Re-doped, (0.04 at% dark brown, 0.09 at% blue, 0.42 at% green, 0.53 at% dark blue with red stars), undoped $IF\text{-}MoS_2$ samples (light brown), $2H\text{-}MoS_2$ (black). Inset: doped and undoped $INT\text{-}WS_2$.

Using the resistivity measurements, the activation energy for ionization of the dopant atoms was calculated by the fluctuating barrier heights model.[9,10] This model used for analyzing the conductivity of polycrystalline semiconductors takes into consideration fluctuations of the barrier heights in the contact points between the different nanoparticles as well as within a single nanoparticle boundary. The results of this analysis indicate that, at 300 K, the activation energy of IF went from approximately 0.35 V for the undoped to less than 0.1 eV for the Re-doped IF. These results are consistent with the theoretical calculations for Re-doped MoS_2 nanotubes which predict a donor level situated 150 meV below the conduction band edge.[11]

Dissipative systems, such as tribological interfaces where static charge accumulation through tribocharging is inevitable, are expected to show clear linkage between their mechanical and electrical properties. Derjaguin and Smilga studied the electrostatic moment of friction between a semi-insulating rod rolling on a metal surface,[12] showing that rolling produces a non-negligible friction component induced by eddy current in the metal surface. In another work, the stick–slip phenomenon between a metallic gold sphere (or graphite rod) shearing on a polyester (insulating) surface was attributed to charge transfer from the polymer surface to the metallic sphere.[13] Using semiconducting IF nanoparticles, such as MoS_2 and WS_2, as additives to lubricating fluids provides a unique handle to study the electronic component of friction and wear.

Tribological measurements using a flat pin (0.09 cm^2) on a disk set-up were carried out using low-viscosity poly(alpha-olefin) (PAO) type 4 (18 MPa s (cSt) at 40°C) fluid and a few measurements were also performed in PAO-6 (32 cSt at 40°C). The results of the experiments are reported in Figure 4. For the PAO-4 experiments, the applied pressure was in the range of 55–66 MPa and the relatively low velocity (0.24 $m s^{-1}$) provided "mixed" lubrication conditions. The friction coefficient in pure oil at the end of the lengthy run-in process was between 0.08–0.1; the temperature was $(40 \pm 3°C)$; the wear rate was 8.5×10^{-7} $mm^3 Nm^{-1}$, and the surface roughness was 1.8 μm. At this point, the IF-oil suspension was added to the interface dropwise. The temperature in the
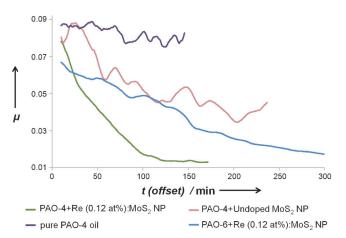
Figure 4. Friction coefficient (μ) versus time measured with pin on disk set-up for different samples in PAO-4 oil. Pin (0.09 cm^2) made of AISI 1020 steel (hardness $H_V = 180$) was rubbed against a disk (AISI 4330 steel; $H_V = 550$). The applied loads are in the range of 500–600 N and the velocity is 0.24 m s^{-1}.

contact area gradually dropped to $30 \pm 3\,°C$. The friction coefficient of PAO-4 with 1 % IF-MoS$_2$ was found to be between 0.04 and 0.05, which is compatible with previous results.[14] Remarkably, the friction coefficient of the oil with 1 wt % Re:IF-MoS$_2$ (0.12 and 0.71 at %) gradually dropped to 0.014–0.016 and the surface roughness parameter decreased from 1.8 to 0.1 µm. Re:IF-MoS$_2$ also exhibits, by-far, the lowest wear rate, 4.7×10^{-8} nm^{3}N^{-1}m^{-1} for 0.12 at % and 2.7×10^{-9} for 0.71 at % Re. In addition, Re-doped IF-WS$_2$ was tested in PAO-6 providing exceedingly low friction coefficient (0.007) and wear rates (1.35×10^{-9} nm^{3}N^{-1}m^{-1}) under similar velocities and load conditions.

The low friction, smooth surface, and the lengthy period of friction in pure oil after the friction test in the oil + Re-doped IF indicate the formation of an easy shear film at the contact surface. The compact film of the Re-doped NP on the tested surface could be seen by SEM and AFM.

It is believed that the agglomeration of the undoped nanoparticles, which hinder their facile access to the interface,[15] is largely alleviated in the case of the doped IF. Furthermore, the reduced friction and wear can be ascribed to the build-up of a film with appreciable conductivity on both sides of the matting metal contact. However more work is required to fully characterize this film and study the tribological mechanism of charged colloidal nanoparticles in oil. These results indicate that both the friction coefficient and the wear rate are adversely affected by tribocharging of the interface, which problem is at least partially relieved by doping the IF.

Most likely, the free carriers are trapped at surface defects inducing negative charge on the NP surface. Such defects occur when the surface monolayer folds in sharp angles and the sulfur atoms are replaced by oxygen or OH moieties in the kinks.[16] The negative surface charge can be balanced by either an inner space-charge layer (band bending); by external double layer or chemisorb positive ions, and possibly jointly by all of these factors. Nonetheless, these surface

charges lead to mutual repulsion at close proximity and prevent agglomeration and subsequent sedimentation of the nanoparticles. Consequently, the nanoparticles can form stable suspensions in the oil. It can also access the tribological interface more easily, providing both easier shearing and a slower wear rate. It should also be recalled that, in the relevant pressure range (up to a few hundred MPa),[17] the free carrier concentration increases with the applied pressure for extrinsically doped metal dichalcogenide semiconductors. Careful doping of the inorganic fullerene-like (IF) NP and nanotubes (INT) could lead to other advances, for example, in the electronic and optical properties of such NP for sensor applications.

[1] a) V. Derycke, R. Martel, J. Appenzeller, P. Avouris, *Appl. Phys. Lett.* **2002**, *80*, 2773; b) J. Kong, C. Zhou, E. Yenilmez, H. Dai, *Appl. Phys. Lett.* **2000**, *77*, 3977; c) C. Zhou, J. Kong, E. Yenilmez, H. Dai, *Science* **2000**, *290*, 1552; d) Y. Cui, X. Duan, J. Hu, C. M. Lieber, *J. Phys. Chem. B* **2000**, *104*, 5213; e) X. Duan, Y. Huang, Y. Cui, J. Wang, C. M. Lieber, *Nature* **2001**, *409*, 66; f) D. J. Bryan, D. R. Gamelin, *Prog. Inorg. Chem.* **2005**, *54*, 47.

[2] L. Krusin-Elbaum, D. Newns, H. Zeng, V. Derycke, J. Sun, R. Sandstrom, *Nature* **2004**, *431*, 672.

[3] V. Ivanovskaya, T. Heine, S. Gemming, G. Seifert, *Phys. Status Solidi B* **2006**, *243*, 1757.

[4] a) Y. Zhu, W. Hsu, S. Firth, M. Terrones, R. Clark, H. Kroto, D. Walton, *Chem. Phys. Lett.* **2001**, *342*, 15; b) F. L. Deepak, R. Popovitz-Biro, Y. Feldman, H. Cohen, A. Enyashin, G. Seifert, R. Tenne, *Chem. Asian J.* **2008**, *3*, 1568.

[5] a) K. Tiong, P. Liao, C. Ho, Y. Huang, *J. Cryst. Growth* **1999**, *205*, 543; b) J. Wildervanck, F. Jellinek, *J. Less-Common Met.* **1971**, *24*, 73.

[6] R. Späh, U. Elrod, M. Lux-Steiner, E. Bucher, S. Wagner, *Appl. Phys. Lett.* **1983**, *43*, 79.

[7] A. Zak, Y. Feldman, V. Alperovich, R. Rosentsveig, R. Tenne, *J. Am. Chem. Soc.* **2000**, *122*, 11108.

[8] V. Petkov, S. J. L. Billinge, J. Heising, M. G. Kanatzidis, *J. Am. Chem. Soc.* **2000**, *122*, 11571.

[9] F. Kopnov, A. Yoffe, G. Leitus, R. Tenne, *Phys. Status Solidi B* **2006**, *243*, 1229.

[10] J. Werner, *Solid State Phenom.* **1994**, *37–38*, 213.

[11] A. N. Enyashin, I. Popov, G. Seifert, *Phys. Status Solidi B* **2009**, *246*, 114.

[12] B. Derjaguin, V. Smilga, *Wear* **1964**, *7*, 270.

[13] R. Budakian, S. Putterman, *Phys. Rev. Lett.* **2000**, *85*, 1000.

[14] R. Rosentsveig, A. Margolin, A. Gorodnev, R. Popovitz-Biro, Y. Feldman, L. Rapoport, Y. Novema, G. Naveh, R. Tenne, *J. Mater. Chem.* **2009**, *19*, 4368.

[15] A. Moshkovith, V. Perfiliev, I. Lapsker, N. Fleischer, R. Tenne, L. Rapoport, *Tribol. Lett.* **2006**, *24*, 225.

[16] C. Shahar, D. Zbaida, L. Rapoport, H. Cohen, T. Bendikov, J. Tannous, F. Dassenoy, R. Tenne, *Langmuir* **2010**, *26*, 4409.

[17] A. Grant, T. Griffiths, G. Pitt, A. Yoffe, *J. Phys. C* **1975**, *8*, L17.